

THE PENNSYLVANIA STATE UNIVERSITY
SCHREYER HONORS COLLEGE

DEPARTMENT OF CHEMICAL ENGINEERING

THE EFFECTS OF pH AND SALT CONCENTRATION ON PROTEIN
FOULING OF VIRE SOLVE PRO VIRUS FILTRATION MEMBRANES

DAVID HOYING
SPRING 2019

A thesis
submitted in partial fulfillment
of the requirements
for a baccalaureate degree
in Chemical Engineering
with honors in Chemical Engineering

Reviewed and approved* by the following:

Andrew Zydney
Professor of Chemical Engineering
Thesis Supervisor

Wayne Curtis
Professor of Chemical Engineering
Honors Adviser

* Signatures are on file in the Schreyer Honors College.

ABSTRACT

Virus filtration plays an essential role as part of the overall viral clearance strategy during the purification of therapeutic proteins. However, one critical problem during virus filtration is protein fouling which results in decreased filtering capacity and economically inefficient purification processes. The objective of this study was to examine the effects of pH and salt concentration on protein fouling during virus filtration through the Viresolve Pro virus filtration membrane. Data were obtained using immunoglobulin G (IgG) as a model protein dissolved in solutions containing 0 mM, 10 mM, 100 mM, and 250 mM KCl at pH 5.5, 7, and 8.5. Filtration was performed at constant transmembrane pressure with the Viresolve Pro membrane oriented in the skin-side down position. At pH 5.5, there was only a weak dependence of the flux on salt concentration, with relatively similar flow rate decays. In contrast, at pH 8.5, the salt free solution showed significantly less protein fouling compared to the solutions containing 10 mM, 100 mM, and 250 mM KCl. Overall, the protein fouling was least during filtration of a salt free solution at pH 8.5, conditions where the IgG is largely negatively-charged. This behavior is consistent with a reduction in protein-membrane interactions due to the presence of electrostatic repulsion between the negatively-charged protein and the negatively-charged membrane. These results provide valuable insights on how solution conditions such as pH and salt concentration can affect the performance of the Viresolve Pro membrane during virus filtration of important bio-therapeutic products.

TABLE OF CONTENTS

LIST OF FIGURES	iii
LIST OF TABLES	iv
ACKNOWLEDGEMENTS	v
Chapter 1 Introduction to Virus Filtration Membranes	1
The Effects of pH on Protein Fouling	2
The Effects of Membrane Orientation on Protein Fouling	3
The Effects of Pressure on Protein Fouling	4
The Effects of Salt Concentration on Protein Fouling	5
Research Objectives	6
Chapter 2 Methods and Materials	7
Solution Preparation	7
Virus Filtration Membrane	8
Protein Fouling Experiments	8
Protein Characterization	9
Chapter 3 Results and Discussion	11
The Effects of pH on Protein Fouling	11
The Effects of Salt Concentration on Protein Fouling	18
Protein Characterization	21
Chapter 4 Conclusions	24
BIBLIOGRAPHY	27

LIST OF FIGURES

Figure 1: Experimental set-up for protein filtration experiments	9
Figure 2: Normalized flow rate at as a function of accumulated filtration volume during filtration of a 1 g/L solution of IgG through the Viresolve Pro membrane at a constant pressure of 30 psi.	11
Figure 3: Normalized flow rate at as a function of accumulated filtration volume during filtration of a 1 g/L solution of IgG at various pH through the Viresolve Pro membrane at a constant pressure of 30 psi.	13
Figure 4: Normalized flow rate at as a function of accumulated filtration volume during filtration of a 1 g/L solution of IgG at various pH containing 10 mM KCl through the Viresolve Pro membrane at a constant pressure of 30 psi.	14
Figure 5: Cumulative Filtrate Volume as a function of pH at a flux decay of 50% for the filtration of 1 g/L IgG in a solution containing 10 mM KCl at various pH through a Viresolve Pro membrane at 30 psi.	15
Figure 6: Normalized flow rate at as a function of accumulated filtration volume during filtration of a 1 g/L solution of IgG at various pH containing 100 mM KCl through the Viresolve Pro membrane at a constant pressure of 30 psi.	15
Figure 7: Cumulative Filtrate Volume as a function of pH at a flux decay of 50% for the filtration of 1 g/L IgG in a solution containing 100 mM KCl at various pH through a Viresolve Pro membrane at 30 psi.	16
Figure 8: Normalized Flow rate as a function of cumulative filtrate volume of a 1 g/L solution of IgG at different pH containing 250 mM KCl through a Viresolve Pro membrane with skin side down at 30 psi.....	17
Figure 9: Normalized flow rate as a function of cumulative filtrate volume of the filtration of a 1 g/L igG solution containing various salt concentration at a pH of 5.5 through a hydrophilic Viresolve Pro membrane with skin side down at 30 psi.	18
Figure 10: Normalized flow rate as a function of Cumulative Filtrate Volume of the filtration of a 1 g/L igG solution containing various salt concentration at a pH of 8.5 through a hydrophilic Viresolve Pro membrane with skin side down at 30 psi.	19
Figure 11: Normalized flow rate as a function of Cumulative Filtrate Volume of the filtration of a 1 g/L igG solution containing various salt concentration at a pH of 7 through a hydrophilic Viresolve Pro membrane with skin side down at 30 psi.	20
Figure 12: Size distribution by volume curve of 5 g/L IgG dissolved in a solution containing 100 mM KCl at various pH.....	21

LIST OF TABLES

Table 1: Average Size by Volume of 5 g/L IgG solution at varying pH and salt concentrations	22
Table 2: Average Zeta Potential of 5 g/L IgG solution at varying pH and salt concentrations	22

ACKNOWLEDGEMENTS

I would like to thank Dr. Andrew Zydney for his guidance and support in pursuing undergraduate research. I would also like to thank Fatemeh Fallahianbijan for all her help designing and setting up the experiments. When I expressed interest to Dr. Zydney about working in his lab, he assigned Fatemeh as my mentor, and she consistently provided help in order for my project to move forward. Dr. Zydney was very committed to helping me be successful in lab. His innovative thought process and extensive knowledge of virus filtration membranes has allowed me to advance as a young researcher.

Chapter 1

Introduction to Virus Filtration Membranes

Virus removal is essential to biopharmaceutical companies in order to ensure that their products can be safely used to treat humans. Virus filtration has become an important component of the overall virus clearance strategy in the production of biopharmaceutical products, with size-exclusion virus filters used to remove small parvoviruses from purified proteins such as human immunoglobulin G or monoclonal antibodies (Bolton et al., 2006). The membranes used in virus filtration typically have a thin, retentive layer with nanoscale-pores that allow the passage of proteins up to 160 kDa in molecular weight while retaining viruses as small as 20 nm (Bolton et al., 2006).

One critical problem that occurs during virus filtration is protein fouling. Protein fouling involves the accumulation of proteins on the surface and / or within the pores of the membrane causing a loss in flux (volumetric flow rate normalized by the membrane area) and a decrease in filter capacity (Bolton et al., 2006). The buildup of proteins can also cause caking on the membrane surface which thickens over time resulting in a reduction of flow rate (Bolton et al., 2006). The resulting loss in capacity can make the filtration economically impractical. However, protein fouling may not only decrease the flow rate, but it may also decrease the membrane's ability to retain viruses (Bolton et al., 2006). Since virus filtration occurs near the end of the downstream purification process, it is highly important that any viruses present are completely removed while achieving very high levels of product recovery. As discussed below, previous

studies indicate that buffer conditions (such as pH and salt concentration), membrane properties, and even membrane orientation can all affect the rate of protein fouling.

The Effects of pH on Protein Fouling

The isoelectric point of a protein is defined as the pH at which the net charge on the protein is zero. If a protein is placed in a solution with a pH above the isoelectric point, it will have a net negative charge due to the dissociation of hydrogen ions from the neutral protein. If the protein is placed in a solution with a pH below the isoelectric point, the protein will have a positive charge due to the protonation of the neutral protein by positively-charged H^+ . Therefore, the use of buffers with varying pH values can alter the electrostatic interactions between the charged membrane and the protein as well as the intermolecular interactions between proteins, both of which can affect the rate and extent of protein fouling.

Bakhshayeshi and Zydney (2007) analyzed the effects of pH on protein fouling of the Viresolve 180 membrane using Bovine serum albumin (BSA), which has an isoelectric point of 4.7, as a model protein. Experiments were performed at pH values of 4.0, 4.7, and 7.0. The data demonstrated that the membrane capacity was significantly reduced near the protein isoelectric point and increased significantly at pH above the isoelectric point, e.g., the capacity at pH 7 was more than eight times that at the protein isoelectric point. The authors hypothesized that this difference was related to differences in the protein mass transfer coefficient, which increased by more than 70% as the pH increased from 4.7 to 7.0 (Bakhshayeshi & Zydney, 2007).

Further research on the effects of pH on protein fouling has been performed by Hadidi

and Zydney (2014) using regenerated cellulose membranes (not virus filters) that are more hydrophilic than the Viresolve 180. Experiments were performed with 5 g/L solutions of IgG, which has an isoelectric point around pH 7. The flux recovery ratios after 1 hour of filtration at pH values of 5, 7, and 9 were 0.84, 0.74, and 0.49, respectively (Hadidi & Zydney, 2014). Thus, fouling was reduced at pH values below the isoelectric point, while, pH values above the isoelectric point actually caused an increase in protein fouling, in sharp contrast to the results from Bakhshayeshi and Zydney (2007) using the Viresolve 180 membrane.

The Effects of Membrane Orientation on Protein Fouling

Most virus filtration membranes are highly asymmetric, with a thin skin layer on top of a support layer with much larger pore size. The membrane can thus be oriented so that the skin-side is facing toward (skin-side-up) or away (skin-side-down) from the protein feed. Virus filtration membranes were originally designed for the skin-side up orientation using tangential flow filtration (Syedain et al., 2006). However, a study performed by Jonsson and Wenten (1994) suggested that normal flow filtration processes using larger pore size microfiltration membranes could be operated with enhanced capacity by reversing the traditional orientation so that the feed enters the large pore size region of the filter first. All virus filters are currently used in the skin-side down orientation using normal flow (or dead end) filtration, with the macroporous support acting as a depth filter that removes large debris before the feed reaches the size-selective skin layer.

Syedain et al. (2006) analyzed the effects of membrane orientation on the fouling characteristics of the Viresolve 180, which is made of hydrophilized polyvinylidene fluoride,

using BSA. Data at a constant pressure of 172 kPa in the skin-side up orientation had a system capacity of 7 L/m², while the system capacity for the skin-side down orientation was 230 L/m² (Syedain et al., 2006). The authors also measured the hydraulic resistance of the fouled membranes using protein-free phosphate buffer solution. The increase in membrane resistance divided by the total protein mass filtered per membrane area for the skin- down orientation was one-fifth of the value obtained for the skin-up orientation (Syedain et al., 2006). The authors hypothesized that the significantly lower resistance in the skin-side down orientation was due to the protein deposits being captured throughout the depth of the membrane while the protein deposits in the skin-side-up orientation are localized primarily on the upper (external) surface of the membrane in a thin compact layer (Syedain et al., 2006).

Bakhshayeshi and Zydney (2007) also showed that the membrane capacity was significantly larger when the membrane was used in the skin-down orientation. The largest increase in membrane capacity was observed at pH 4 with the capacity being 20-fold greater than that in the skin-side down orientation under these conditions (Bakhshayeshi and Zydney, 2007).

The Effects of Pressure on Protein Fouling

One factor that must be considered when running a virus filtration process is the operating pressure. Prior to 2011, high pressure was assumed to be the worst operating conditions for virus clearance (Strauss et al., 2017). However, Blumel et al. (2013) found that low transmembrane pressure can negatively impact a virus filtration membrane's ability to remove parvoviruses. Operating pressure not only affects the membrane's ability to remove viruses, but it also effects the filtering capacity due to changes in protein fouling.

Syedain et al. (2006) evaluated the effects of pressure on fouling of the Viresolve 180 membranes oriented either skin-side up or skin-side down using 1 g/L solutions of BSA. For the skin-side up orientation, the system capacity at constant pressures of 69, 103, and 172 kPa were 41, 13, and 7 L/m², respectively. This shows that there is a significant decrease in filtering capacity as the pressure of the system is increased for the skin-side up orientation. Experiments performed at constant filtrate flux showed that reducing the flux from 32 to 25 μm/s resulted in a 4-fold increase in system capacity (Syedain et al., 2006). The fouling mechanism was also analyzed by scanning electron microscopy, which showed that most of the membranes pores remained open even after fouling with BSA, suggesting that the flux decay observed at a constant pressure may not be due to irreversible fouling.

The Effects of Salt Concentration on Protein Fouling

Protein-protein interactions drive many biophysical processes such as aggregation, solubility, and phase transitions. During virus filtration, it is important to prevent protein aggregation in order to avoid the blockage of membrane pores due to protein fouling of the membrane. Since electrostatic repulsion between like-charged proteins decreases as the salt concentration is increased, protein aggregation also tends to increase at high salt concentrations (Tsumoto et al., 2007).

There is very little research on the effects of salt concentration on the performance of virus filtration membranes. However, the effects of salt concentration on protein fouling has been previously examined during the use of polyvinylidene fluoride ultrafiltration membranes that have smaller pores than virus filters. Gao et al. (2018) analyzed the effects of ionic strength

on BSA fouling at a pH of 7.5 and a protein concentration of 100 mg/L. After 100 minutes of filtration, the flux decline was significantly larger when BSA had no salt present compared to that with 100 mM NaCl (Gao et al., 2018). However, after 400 minutes of filtration, the flux decline was larger with the 100 mM NaCl solution. This unusual dependence on salt concentration may be due to a salting-out phenomenon that could occur at the high salt concentration near the membrane surface (Gao et al., 2018).

Research Objectives

The overall goal of this thesis is to provide a more complete understanding of the factors that control protein fouling during protein filtration through the Viresolve Pro virus filtration membranes, a relatively new membrane that shows very high performance in terms of virus retention.

The details of the general experimental methods used in this work are described in Chapter 2. Chapter 3 provides results for the flux decline during filtration over a range of buffer conditions. Chapter 4 discusses the key findings and some of the implications of this work for the development of effective virus removal filtration processes in the production of biopharmaceutical products used to treat various diseases.

Chapter 2

Methods and Materials

Solution Preparation

Solutions of 0, 10, 100, and 250 mM KCl were prepared by dissolving pre-weighed amounts of KCl (J.T Baker, Philipsburg, NJ) in deionized distilled water obtained from a Millipore water purification system (Direct-Q 3UV-R) with a resistivity greater than 18 M Ω -cm. Solutions were buffered with sodium acetate (EM Science, Gibbstown, NJ) for pH 5.5, tris(hydroxymethyl)aminomethane (OmniPur, Gibbstown, NJ) for pH 8.5, and Bis-tris (MP Biomedicals, LLC, Solon, OH) for pH 7. The pH was adjusted using 1 M HCl or KOH as required and was measured with a model pH 700 Oakton pH meter (Oakton, Vernon Hills, IL). All buffer solutions were filtered through 0.22 μ m pore-size sterile filters (Millipore Corp., Bedford, MA) to remove any particles or undissolved salt before use.

Immunoglobulin G (IgG) from SeraCare Life Sciences (Milford, MA) was used as a model protein due to the current interest in virus filtration of monoclonal antibodies (a type of immunoglobulin) and the available previous research on IgG fouling. The SeraCare IgG contains approximately 16.3% dimers and a small percentage of trimers. Protein solutions of 2 g/L were prepared by dissolving the appropriate mass of powdered IgG in the desired buffered salt solution; these were diluted with additional buffer to obtain a final protein concentration of 1 g/L. Protein solutions were prepared fresh for each filtration experiment. All protein solutions were filtered through a 0.22 μ m VWR syringe filter (VWR, Radnor, PA) to remove any large protein aggregates prior to use. Protein concentrations were analyzed by using a UV-vis

spectrophotometer (NanoDrop 2000c, Thermo Scientific, Waltham, MA) with the absorbance measured at 280 nm.

Virus Filtration Membrane

All filtration experiments were performed using Viresolve Pro membranes (Millipore Corp., Billerica, MA). The Viresolve Pro membrane has a composite structure made of a hydrophilized polyethersulfone. The membrane has a thin-skin layer that allows for virus retention and provides high transmission of proteins like IgG. Immediately before the experiment, the membrane was washed with 100 mL of deionized distilled water obtained from a Millipore Ultrapure water purification system (Direct-Q 3UV-R) with a resistivity greater than 18 M Ω -cm. A single new membrane was used for each protein fouling experiment.

Protein Fouling Experiments

All filtration experiments were conducted in a stainless-steel filtration cell (Model XX4404700, Millipore Corp., Bedford, MA) using the experimental set-up shown in Figure 1. Membranes were cut into 47 mm disks from a large flat sheet using a specifically designed cutting device. A 47-mm diameter GVS Nylon spacer (pore size of approximately 5 μ m) was placed immediately beneath the membrane to minimize pore blockage by the stainless-steel support. Data were obtained with the membrane oriented so that the skin-side was facing down away from the feed as per the manufacturer's recommendation.

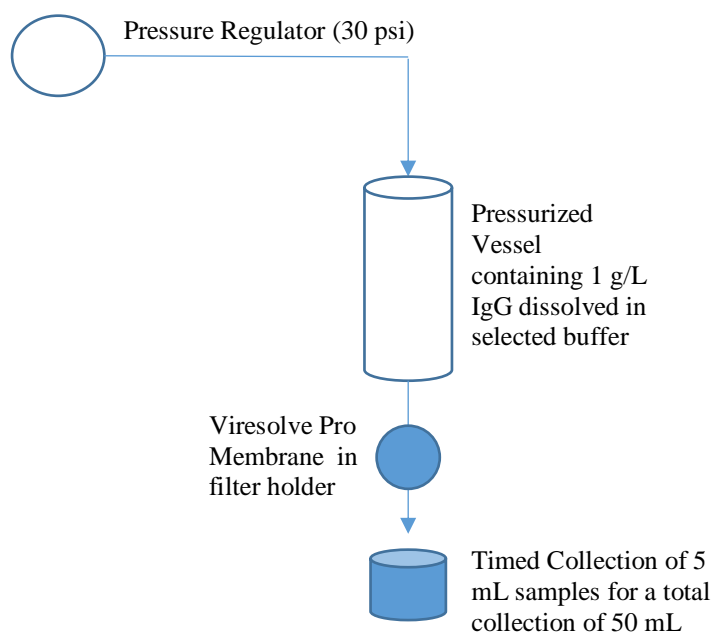


Figure 1: Experimental set-up for protein filtration experiments

The feed reservoir was filled with the desired solution and air-pressurized to obtain a gauge pressure of 30 psig (210 kPa). Filtrate flow rate was measured by timed collection using a digital balance (PG802-S, Mettler Toledo, Columbus, OH). The feed reservoir was initially filled with 40 mL of the selected buffered salt solution, with the buffer flow rate measured to evaluate the membrane permeability. The feed reservoir was then emptied and refilled with a 1 g/L protein solution at the desired pH, re-pressurized to 30 psig, and the protein filtration experiment was started. All experiments were performed at room temperature.

Protein Characterization

The desired amount of IgG was pre-weighed to obtain a protein concentration of 5 g/L in the desired buffer and stirred at low speed for 24 hours. The protein solution was then centrifuged at 3800 g for approximately 20 minutes to remove any insoluble material. The

supernatant was collected and filtered through a 0.2 μm pore size syringe filter (VWR, Radnor, PA). The protein sample was then analyzed using the Zetasizer Nano-ZS90 (Malvern, Westborough, MA) to evaluate both the size distribution and zeta potential. The quartz cell (QS Cuvette, DTS2145) was first washed with deionized distilled water and then ethanol, with that process repeated several times. The protein solution was then added to the quartz cell for analysis by dynamic light scattering and electrophoretic mobility.

Chapter 3

Results and Discussion

The Effects of pH on Protein Fouling

Typical experimental data for filtrate flow rate during a constant pressure filtration experiment performed at a transmembrane pressure of 30 psig during filtration of 1 g/L IgG dissolved in a solution containing 0 mM KCl at pH 8.5 through a Viresolve Pro membrane with the skin-side down are shown in Figure 2.

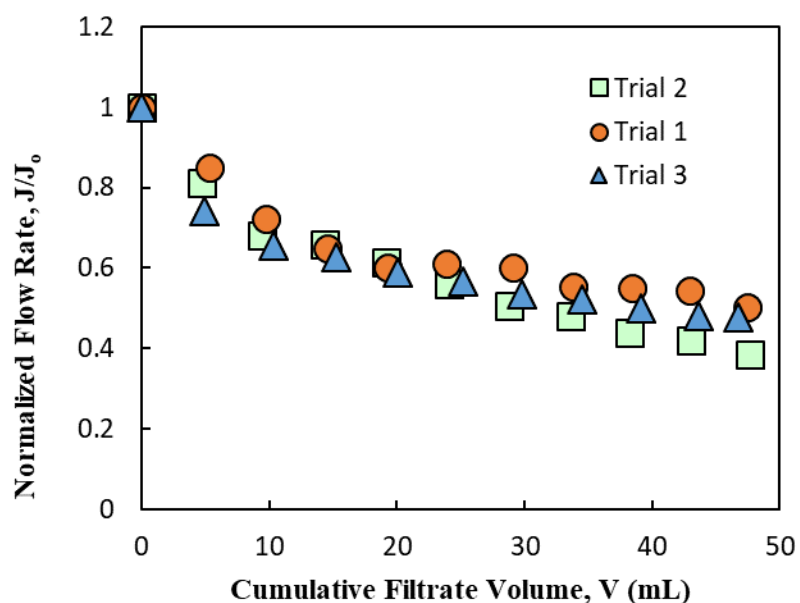


Figure 2: Normalized flow rate at as a function of accumulated filtration volume during filtration of a 1 g/L solution of IgG through the Viresolve Pro membrane at a constant pressure of 30 psi.

The buffer flow rates through the 3 membranes evaluated immediately before the IgG filtration were nearly identical with values ranging from 0.35 to 0.38 mL/s. The data are plotted as the normalized flow rate, defined as the measured flow rate divided by the flow rate of the buffer

(containing no protein) through the fresh membrane. The results are shown as a function of the cumulative filtrate volume for experiments performed up to a total of 50 mL (corresponding to a throughput of 29 L/m² of membrane area). Data from 3 repeat experiments under the same conditions showed good reproducibility, with the filtrate flow rate declining by approximately 50% over the course of the filtration. Experimental data for the IgG concentration in the filtrate samples obtained periodically during the course of the filtration showed minimal IgG retention by the Viresolve Pro as expected.

Experimental data at a pH 5.5 and 8.5 containing 0 mM KCl are compared in Figure 3. In both cases, the flow rate rapidly decreased rapidly to approximately 60% of its initial value after a cumulative filtrate volume of 20 mL. However, the flow rate at pH 8.5 shows a lower rate of flux decline over the latter half of the filtration while the flow rate for the IgG at pH 5.5 shows a more continuous decay to a value of only 40% of the initial flow after 43 mL. The difference in flow rate decay is small between pH 5.5 and 8.5 under these conditions, suggesting that the fouling of a positively charged (pH 5.5) or a negatively charged (pH 8.5) IgG protein in the absence of salt is very similar.

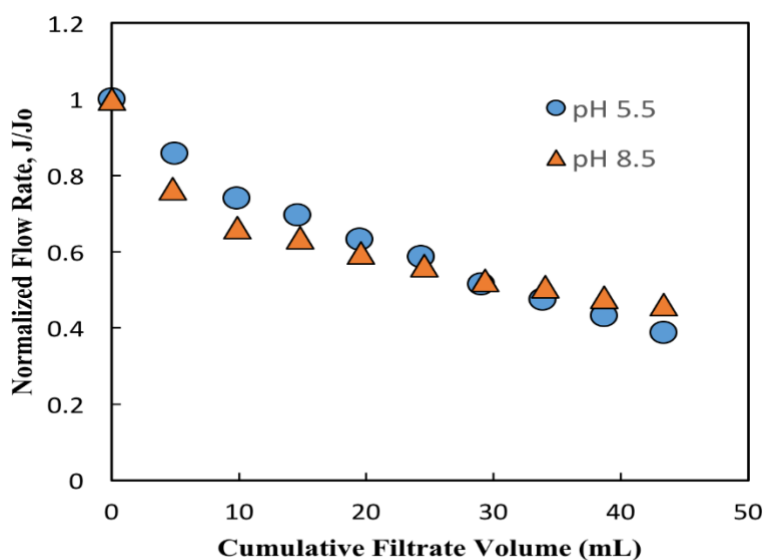


Figure 3: Normalized flow rate at as a function of accumulated filtration volume during filtration of a 1 g/L solution of IgG at various pH through the Viresolve Pro membrane at a constant pressure of 30 psi.

Corresponding data for the filtration of 1 g/L solutions of IgG in 10 mM KCl are shown in Figure 4. The buffer flow rates through the 3 membranes were all in the range of 0.41 to 0.45 mL/s, with no apparent dependence on the solution pH. In this case, the degree of fouling during IgG filtration increased significantly as the pH is increased. The lowest amount of flux decline is seen at pH 5.5, with the flow rate decreasing by slightly more than 60% after filtration of 44 mL. In contrast, the same degree of flux decline is seen at pH 7 after about 22 mL and at pH 8.5 after less than 15 mL. However, the flow rate at pH 7 begins to level off in the latter half of the filtration to the same final flux decay as at pH 8.5 after a cumulative filtrate volume of 47 mL. The final flux decline also showed significant differences at the different pH values, with the filtrate flux at pH 8.5 and 7 decreasing by more than 85% while that at pH 5.5 decreased by only 60%.

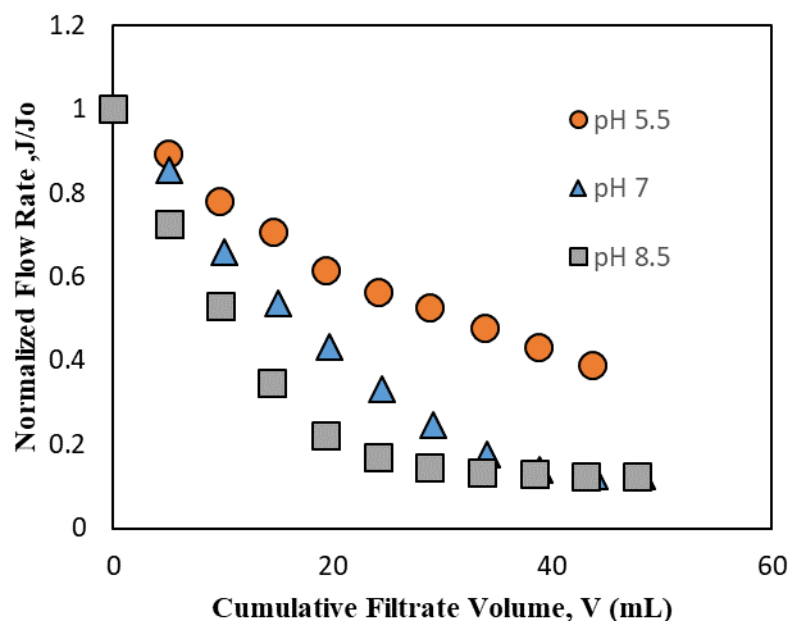


Figure 4: Normalized flow rate as a function of accumulated filtration volume during filtration of a 1 g/L solution of IgG at various pH containing 10 mM KCl through the Viresolve Pro membrane at a constant pressure of 30 psi.

The effect of pH on the cumulative filtrate volume is shown more explicitly in Figure 5. The data are plotted as the cumulative filtrate volume at a flux decay of 50%, with the value of V determined by linear interpolation of the flow rate data shown in Figure 4. The symbols represent results obtained in repeat experiments under identical conditions, all in 10 mM KCl solutions. The repeat experiments show good reproducibility at pH 5.5 and pH 7 with somewhat larger variation at pH 8.5. The cumulative filtrate volume at a flux decay of 50% decreases sharply with increasing pH, going from a value of nearly 25 mL at pH 5.5 to as low as 10 mL at pH 8.5, i.e., as the IgG goes from being positively-charged to negatively-charged. The higher capacity at pH 5.5 is surprising given that there should be attractive electrostatic between the positively charged IgG and the negatively-charged Viresolve Pro membrane at pH 5.5.

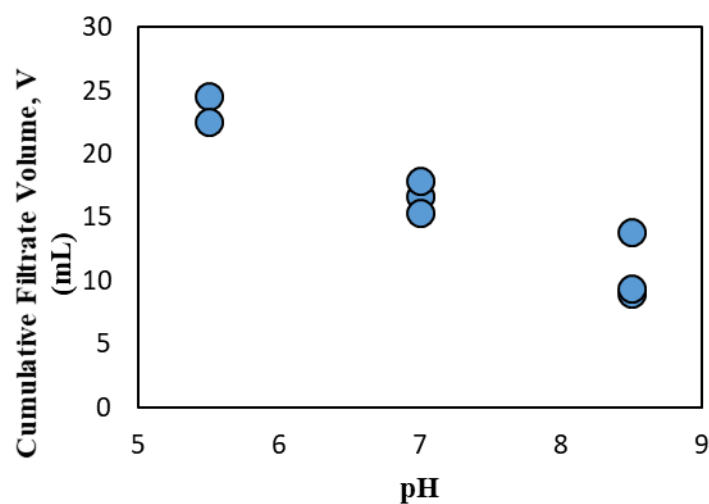


Figure 5: Cumulative Filtrate Volume as a function of pH at a flux decay of 50% for the filtration of 1 g/L IgG in a solution containing 10 mM KCl at various pH through a Viresolve Pro membrane at 30 psi.

The flow rate decay for 1 g/L IgG solutions in 100 mM KCl are shown in Figure 6. The smallest flux decline is again obtained at pH 5.5, but in this case the greatest flux decline is seen at pH 7. The flow rate decreases by approximately 80%, 95%, and 85% at pH 5.5, pH 7, and pH 8.5 respectively. Therefore, the greatest flux decay occurs at the isoelectric point of IgG during the filtration of solutions containing 100 mM KCl.

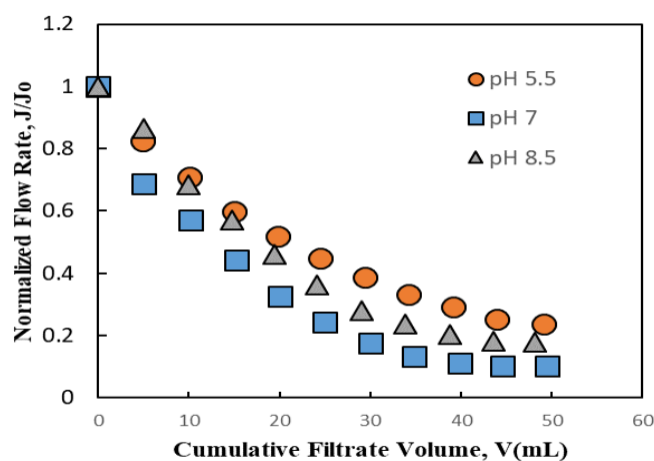


Figure 6: Normalized flow rate at as a function of accumulated filtration volume during filtration of a 1 g/L solution of IgG at various pH containing 100 mM KCl through the Viresolve Pro membrane at a constant pressure of 30 psi.

The final values of the normalized flow rate in the 100 mM KCl solutions at pH 5.5 are well below the corresponding values obtained in the 10 mM KCl solutions. In contrast, the final filtrate flow rate decreased by 80% at pH 8.5 which is slightly less than the 90% decrease observed in the 10 mM KCl solution.

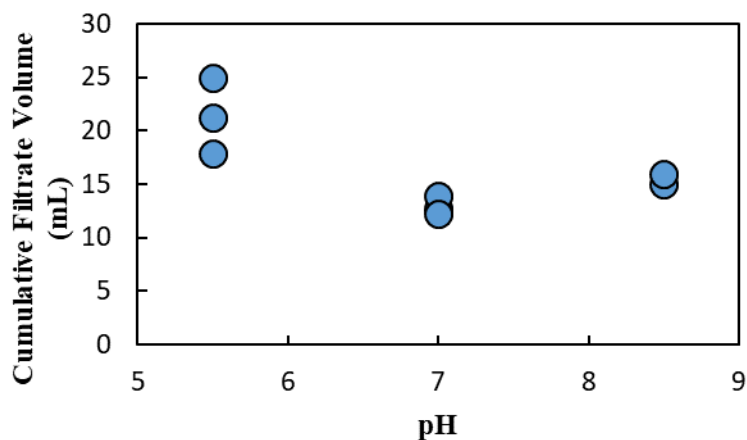


Figure 7: Cumulative Filtrate Volume as a function of pH at a flux decay of 50% for the filtration of 1 g/L IgG in a solution containing 100 mM KCl at various pH through a Viresolve Pro membrane at 30 psi.

Figure 7 shows the cumulative filtrate volume as a function of solution pH for the data in the 100 mM KCl solutions. Three repeat experiments were performed at each pH, with the greatest scatter in the data seen at pH 5.5. The cumulative filtrate volume clearly displays a minimum value at pH 7, with the largest filtrate volume obtained at pH 5.5. In contrast, the minimum cumulative filtrate volume for the filtration of the 1 g/L IgG in the 10 mM KCl solutions was at pH 8.5 (Figure 5). The reduction in fouling when operating at a pH above or below the isoelectric point of IgG is consistent with previous observations by Bakhshayeshi and Zydney (2007).

Experimental results for 1 g/L solutions of IgG in 250 mM KCl are shown in Figure 8.

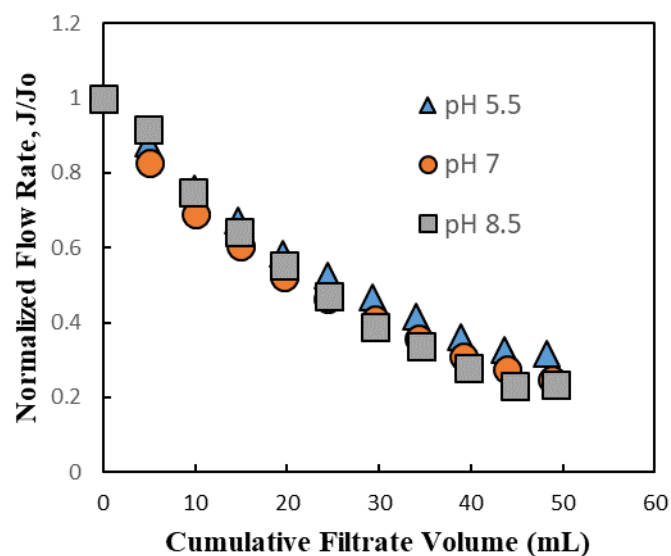


Figure 8: Normalized Flow rate as a function of cumulative filtrate volume of a 1 g/L solution of IgG at different pH containing 250 mM KCl through a Viresolve Pro membrane with skin side down at 30 psi

In this case, the flow rate decay is approximately the same at all 3 pH values, suggesting that the use of the 250 mM KCl reduces the effects of electrostatic interactions. Therefore, at high salt concentrations, the effect of pH on protein fouling is essentially negligible.

The Effects of Salt Concentration on Protein Fouling

The effect of salt concentration on IgG fouling is examined more explicitly in Figures 9 to 11.

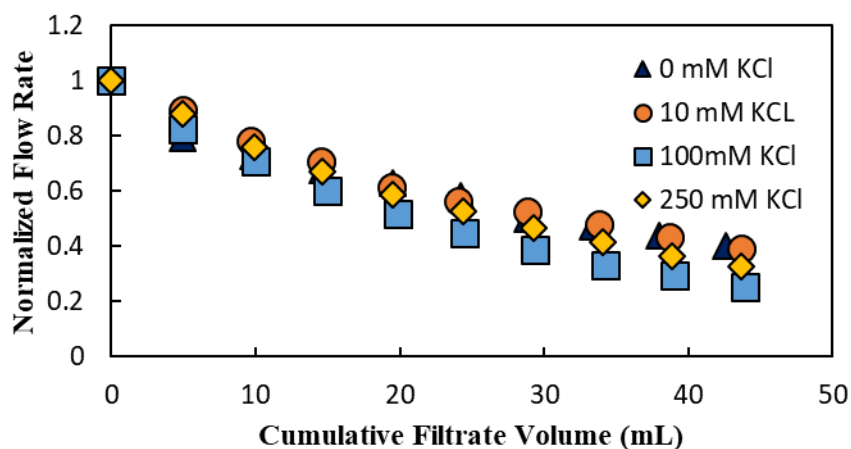


Figure 9: Normalized flow rate as a function of cumulative filtrate volume of the filtration of a 1 g/L IgG solution containing various salt concentration at a pH of 5.5 through a hydrophilic Viresolve Pro membrane with skin side down at 30 psi.

The results at pH 5.5 (Figure 9) show a relatively weak dependence on the KCl concentration, with the highest rate of protein fouling seen at a salt concentration of 100 mM. In contrast, the data at pH 8.5 (Figure 10) show a very strong dependence of fouling on the salt concentration.

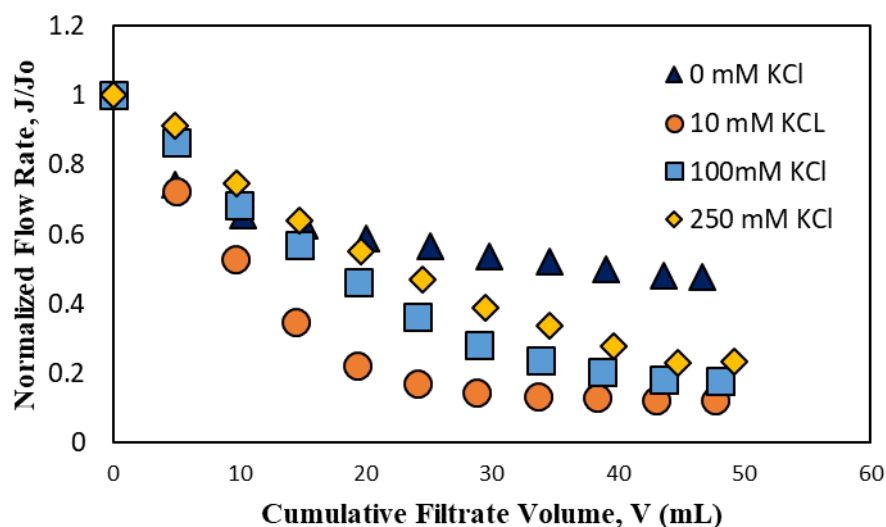


Figure 10: Normalized flow rate as a function of Cumulative Filtrate Volume of the filtration of a 1 g/L igG solution containing various salt concentration at a pH of 8.5 through a hydrophilic Viresolve Pro membrane with skin side down at 30 psi.

In this case, the least flux decline is seen in the salt free solution, with the greatest amount of fouling occurring at a salt concentration of 10 mM KCl. The final flow rate values were 23%, 18%, and 12% of the initial values at salt concentrations of 250 mM, 100 mM, and 10 mM KCl, respectively. Therefore, neglecting the salt free solution, it appears that less protein fouling occurs at higher salt concentrations at pH 8.5. The origin of this unusual dependence of fouling on the salt concentration is unclear.

The effect of KCl concentration on the filtration of 1 g/L solutions of IgG through the Viresolve Pro membranes at pH 7 are summarized in Figure 11.

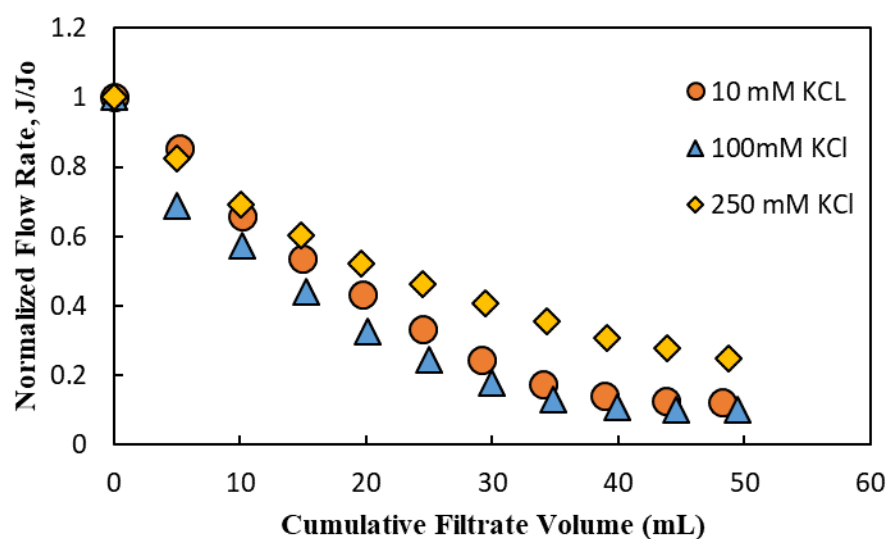


Figure 11: Normalized flow rate as a function of Cumulative Filtrate Volume of the filtration of a 1 g/L igG solution containing various salt concentration at a pH of 7 through a hydrophilic Viresolve Pro membrane with skin side down at 30 psi.

The data at 10 and 100 mM KCl show nearly identical rates of flow decay, with the normalized flow rate decreasing to approximately 10% of its initial value in both salt solutions at a cumulative filtrate volume of 50 mL. In contrast, much less fouling is seen in the 250 mM KCl solution, with the final flow rate only decreasing by about 75% over the course of the filtration. The decrease in protein fouling during the filtration of solutions containing 250 mM KCl compared to those with 10 mM and 100 mM KCl is observed at both pH 7 (Figure 11) and pH 8.5 (Figure 10).

Protein Characterization

In order to understand the effects of solution conditions on the fouling behavior, the protein size and zeta potential were evaluated under the different pH and salt concentrations.

Figure 12 shows a typical size distribution by volume for solutions of 5 g/L IgG in 100 mM KCl at various pH.

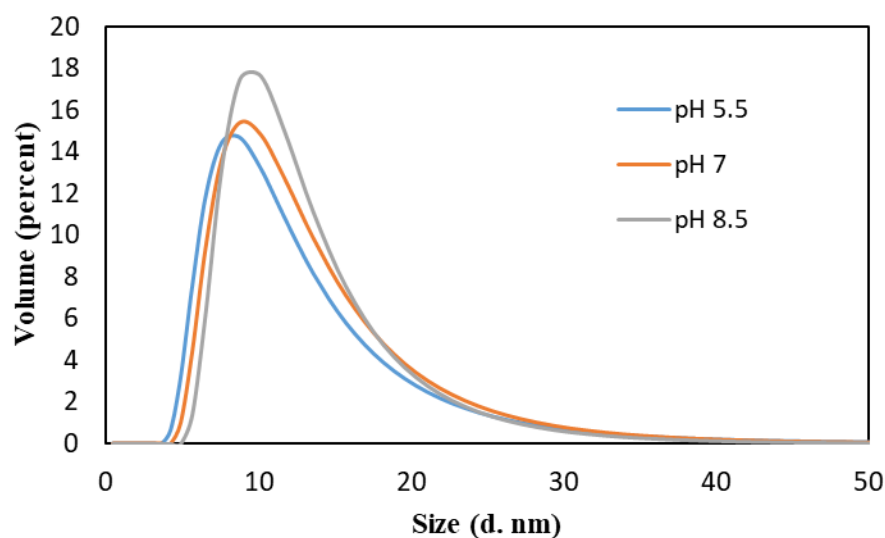


Figure 12: Size distribution by volume curve of 5 g/L IgG dissolved in a solution containing 100 mM KCl at various pH

There was no evidence of any large aggregates in any of the DLS data. The mean size of the IgG was between 11 and 12 nm at all three pH values, although the curve at pH 8.5 does appear to be shifted to slightly larger size.

Table 1 summarizes the protein size data collected by dynamic light scattering at various pH and salt concentrations. The average protein size varied from 11.8 to 12.7 nm, with no statistical differences in the values (the estimated error on the measured size was approximately 5 nm). The data in the 10 mM KCl solution do show a slight increase in effective size with increasing pH, which is consistent with the observed decrease in capacity (cumulative filtrate

volume) with increasing pH seen previously in Figure 4. Similarly, the data in the 100 mM KCl solution show the largest size at pH 7, which is the pH that yielded the lowest cumulative filtrate volume (largest degree of fouling). However, these differences in size were too small to draw any quantitative conclusions on the effects of IgG size on the fouling behavior.

Table 1: Average Size by Volume of 5 g/L IgG solution at varying pH and salt concentrations

Average protein size by volume		
pH	10 mM KCl	100 mM KCl
5.5	12.2 nm	12.0 nm
7	12.6 nm	12.1 nm
8.5	12.7 nm	11.8 nm

The protein zeta potential was also evaluated at the various pH and salt concentrations, with the results summarized in Table 2.

Table 2: Average Zeta Potential of 5 g/L IgG solution at varying pH and salt concentrations

Average Zeta Potential (mV)		
pH	0 mM KCl	10 mM KCl
5.5	8.7 ± 4.3	5.8 ± 7.1
7	4.9 ± 3.0	1.8 ± 3.8
8.5	-2.6 ± 3.0	-4.2 ± 7.2

The zeta potential of IgG decreased with increasing pH as expected, with the protein having a positive charge at pH 5.5 and a negative charge at pH 8.5. The charge values in the 10 mM KCl solution were similar to those in the absence of any KCl, with the largest difference seen at pH 7, i.e., near the protein isoelectric point. Note that it was not possible to evaluate the

zeta potential in the 100 and 250 mM KCl solutions due to the very small values of the electrophoretic mobilities under these conditions.

Chapter 4

Conclusions

This thesis examined the effects of pH and salt concentration on the fouling characteristics of IgG during filtration through a Viresolve Pro virus removal membrane oriented in the skin-side down position. The lowest rate of protein fouling occurred at a pH of 8.5 and a salt free solution, with the flow rate declining by slightly more than 50% after a cumulative filtrate volume of 47 mL (corresponding to 27 L/m² of membrane area). The low level of fouling observed under these conditions is likely due to repulsive electrostatic interactions between the negatively-charged IgG and the negatively-charged Viresolve Pro membrane at this high pH. The low ionic strength of the IgG solution (no added KCl) would enhance these repulsive interactions, minimizing the adhesion of the IgG to the membrane surface.

The highest rate of protein fouling occurred at a pH of 7 and a salt concentration of 100 mM KCl although a very similar degree of fouling was seen in the 10 mM KCl solution at this same pH. The IgG is relatively un-charged at pH 7, which tends to destabilize the protein; previous studies have also shown maximum fouling near the protein isoelectric point for other types of membrane filters. Interestingly, the degree of fouling at pH 7 in the presence of 250 mM KCl was reduced compared to that in the 10 and 100 mM KCl solutions. The origin of this improved filtration behavior is unclear since high salt concentrations would be expected to have relatively little effect on protein fouling near the protein isoelectric point.

The lowest rate of fouling for solutions containing salt concentrations of 10 mM, 100 mM, and 250 mM KCl was at pH 5.5 (compared to that at pH 7 and pH 8.5). This may suggest that IgG filtration is more favorable (less fouling) when the IgG is positively-charged, i.e., at a pH below the protein isoelectric point. However, it is important to note that the isoelectric point of the Viresolve Pro membrane is probably around pH 5; thus, the lack of fouling seen under these conditions could be related to the absence of any significant charge on the membrane surface, which would minimize electrostatic interactions between the protein and the membrane surface.

Experiments performed at a salt concentration of 250 mM KCl showed nearly identical flow rate decay at pH 5.5, 7, and 8.5, which is consistent with the absence of any significant electrostatic interactions at high salt concentrations due to the strong electrostatic shielding by the KCl. These results confirm the importance of electrostatic interactions in governing the fouling behavior during protein filtration through virus removal membranes.

Zeta potential and light scattering data were used to characterize the IgG in the different pH / salt solutions. The zeta potential results confirmed that the serum IgG used in this work had an isoelectric point slightly above pH 7, consistent with results obtained by previous studies. Dynamic light scattering data showed no significant differences in IgG size in the different solutions, indicating that protein aggregation in the bulk solution (governed by intramolecular interactions between IgG molecules) was unlikely to be the cause of the different fouling behavior seen at the different pH and salt concentrations.

Future experimental studies should consider other methods for protein characterization and for quantifying the interactions between the protein and membrane surface. Size exclusion

chromatography could likely provide greater insights into the formation of protein dimers and small oligomers in the different pH and salt concentration solutions; these small oligomers could well play a major role in protein fouling given the 20 nm pore size of the Viresolve Pro membrane. It might also be possible to use atomic force microscopy (AFM) to map the surface charge characteristics of the membrane. In principle, one could use an AFM probe with immobilized IgG on the tip of the AFM to measure the longer range interactions between the IgG and the Viresolve Pro membrane under different solution conditions. It would also be useful to extend these studies to examine other virus filtration membranes with different surface charge characteristics. For example, the Planova 20N virus filter is a cellulosic membrane and is relatively uncharged over a broad range of pH. This might allow one to more effectively probe the effects of the protein charge on membrane fouling since the membrane charge would be largely constant.

The results from this research do provide valuable information on the protein fouling characteristics of the Viresolve Pro membrane, one of the most widely used virus filtration membranes used in the biopharmaceutical industry. The experimental data at pH 5.5 demonstrate that it may be possible to significantly increase the capacity, i.e., reduce the extent of fouling, by performing the virus filtration at pH below the isoelectric point of the protein in solutions at moderate ionic strength, while the data at pH 8.5 with no added salt show even less fouling. The research presented in this thesis should provide a solid foundation for future studies to improve the use of virus filtration membranes in the purification of high value biopharmaceutical products that are widely used for the treatment of a wide range of important diseases.

BIBLIOGRAPHY

- Bakhshayeshi, M., & Zydney, A.L. 2007. Effect of solution pH on protein transmission and membrane capacity during virus filtration. *Biotechnology and Bioengineering*, 100, 108-117.
- Bolton, G.R., Spector, S., & Lacasse, D. 2006. Increasing the capacity of parvovirus-retentive membranes: Performance of the Viresolve Prefilter. *Biotechnology and Applied Biochemistry*, 43, 55-63.
- Gao, F., Wang, J., Zhang, H., Jia, H., Cui, Z., & Yang, G. 2018. Role of ionic strength on protein fouling during ultrafiltration by synchronized UV-Vis spectroscopy and electrochemical impedance spectroscopy. *Journal of Membrane Science*, 563, 592-601.
- Hadidi, M., & Zydney, A.L. 2014. Fouling behavior of zwitterionic membranes: Impact of electrostatic and hydrophobic interactions. *Journal of Membrane Science*, 452, 97-103.
- Jonsson, G. E. & Wenten, I. G. 1994. Control of concentration polarization, fouling and protein transmission of microfiltration processes within the agro-based industry. *Proceedings ASEAN-EC Workshop on Membrane Technology in Agro-based Industry*, 157–166.
- Strauss, D., Goldstein, J., Hongo-Hiraski, T., Yokoyama, Y., Hiroto, N., Miyabayashi, T., & Vacante, D. 2017. Characterizing the impact of pressure on virus filtration processes and establishing design spaces to ensure effective parvovirus removal. *Biotechnology Progress*, 33, 1294-1302.

- Syedain, Z.H., Bohonak, D.M., & Zydney, A.L. (2006). Protein fouling of virus filtration membranes: Effects of membrane orientation and operating conditions. *Biotechnology Progress*, 22, 1163-1169.
- Tsumoto, K., Ejima, D., Senczuk, A.M., Kita, Y., & Arakawa, T. 2007. Effects of salts on protein-surface interactions: applications for column chromatography. *Journal of Pharmaceutical Sciences*, 96, 1677-1690
- Wilkommen, H., Blumel, J., Brorson, K., Chen, D., Chen, Q., Groner A., Kreil TR, Robertson J.S., Ruffing, M., & Ruiz, S. 2013. Meeting report- workshop on virus removal by filtration: Trends and new developments, 2011 PDA Virus and TSE Safety Forum. *PDA Journal of Pharmaceutical Science and Technology*. 98-104.

ACADEMIC VITA

DAVID R. HOYING

The Pennsylvania State University | Class of 2019 | Cell: (216) 870-3495 | Email: drh5388@psu.edu

EDUCATION

The Pennsylvania State University, University Park, PA Present - May 2019

Bachelor of Science in Chemical Engineering

Dean's List: 7/7 semesters

Larry B. Parsons Scholarship Recipient for High Achieving Chemical Engineering Students

Schreyer Honors College- *Thesis Title*: "The Effects of pH and Salt Concentration on Protein Fouling of Viresolve Pro Virus Filtration Membranes"

WORK EXPERIENCE

Merck Vaccine Process Development Intern, West Point, PA Summer 2018

Vaccine Process Development Intern

- Executed purification experiments using chromatography systems such as AKTA PCC and AKTA Explorer
- Conducted dynamic binding capacity experiments to analyze viral breakthrough
- Analyzed chromatograms obtained from Unicorn and dynamic light scattering
- Performed virus capture experiments with Anion-Exchange (AEX) Chromatography using Simulated
- Moving Bed Technology
- Presented data on large particle Simulated Moving Bed Technology to executives of bio-processing
- Collaborated with a team of engineers and biochemists to develop experimental methods

Bioprocessing and Membrane Separations Lab, University Park, PA 2018-Present

Undergraduate Researcher

- Developed experiments to test protein fouling effects on virus filtration using VPro membrane
- Calculated and analyzed protein concentration and flow rates during membrane filtration
- Researched mechanisms involved in protein aggregation causing protein fouling

Department of Biochemistry and Molecular Biology, University Park, PA 2016 - 2018

Undergraduate Researcher

- Developed mutations in the Spt5 through In-fusion reactions
- Analyzed PCR products on agarose gel
- Transformed DNA plasmids into Rosetta (DE3 pLysS) competent cells
- Performed protein purification with Flag-tagged and Talon Resin columns
- Analyzed SDS-PAGE gels to detect if mutated proteins were present after each purification step

College of Engineering Initiative Research Program (CERI), Penn State Spring 2017

Student Member and Scholarship Recipient

- Managed and collaborated with primary investigator on own research project
- Required 10 hours of research per week and a research paper
- Presented research at the University Wide Undergraduate Research Exhibition

Swagelok Summer Internship Program, Solon, OH

Summer 2017

Continuous Improvement Lab Intern

- Performed quality testing on various fluid-system fittings to make sure product reached
- catalogued working pressure
- Developed guidelines to produce an equipment health number to perform a risk analysis on lab equipment
- Created a matrix with equipment health number data to be used for capital expenditure planning
- Flow tested competitor valves and analyzed Cv values for a Product Engineer Team
- Presented projects to top executives during a company conference

RELEVANT ENGINEERING PROJECTS**Engineering Design of Healthcare Prototype, Tecnum University**

Summer 2016

Student Designer

- Worked with Spanish and Penn State students to create a wearable prototype
- Designed functioning prototype of a foot insole that incorporated a pressure sensor at the heel
- Met requirement that wearable prototype would be used to benefit consumers' health